

NANO EXPRESS

Open Access



Hydrothermal Synthesis of ZnO Structures Formed by High-Aspect-Ratio Nanowires for Acetone Detection

Zhen Cao¹, Yong Wang^{2*}, Zhanguo Li² and Naisen Yu^{3*}

Abstract

Snowflake-like ZnO structures originating from self-assembled nanowires were prepared by a low-temperature aqueous solution method. The as-grown hierarchical ZnO structures were investigated by X-ray diffraction (XRD) and field-emission scanning electron microscopy (FESEM). The results showed that the snowflake-like ZnO structures were composed of high-aspect-ratio nanowires. Furthermore, gas-sensing properties to various testing gases of 10 and 50 ppm were measured, which confirms that the ZnO structures were of good selectivity and response to acetone and could serve for acetone sensor to detect low-concentration acetone.

Keywords: ZnO, Snowflake-like structures, Acetone Detection

Background

As wide band gap materials, ZnO has been widely investigated for its potential applications [1–9]. Especially, it can be used in toxic and combustible gas detectors [10–13]. For gas sensor applications, ZnO is one of the promising materials. Moreover, low-dimensional ZnO materials have a large surface-to-volume ratio, which can be used as a potential material on gas-sensing devices [14–20]. ZnO nanostructures with different morphologies have been synthesized through a wide range of preparation methods [21, 22]. Among these methods, the low-temperature route is a suitable choice because of its simplicity, reproducibility, and cost-effectiveness and is attracting considerable attention [23, 24].

Acetone is a commonly used chemical solvent, which has been regarded as an extracting reagent in the industry. In addition, acetone is a very important marker for noninvasive diagnosis of diabetes in the human breath aspects [25]. Thus, it is of great significance to develop a new type of acetone gas sensor that can be used as a non-invasive detector. The use of low-dimensional structures

is a key technological factor in the creation of new functional and sensing devices [26].

We proposed a low-temperature method to prepare snowflake-like ZnO structures in this paper. The structures and morphologies have been investigated by X-ray powder diffraction (XRD) and field-emission scanning electron microscopy (FESEM). Micro-Raman and absorption spectrum were also performed to investigate the optical properties of the structures. Meanwhile, a gas sensor was made basing on the snowflake-like ZnO structures, and its gas-sensing properties were investigated. Particularly, the prepared sensor exhibited good selectivity and response to acetone which makes it as a good candidate for detecting low-concentration acetone.

Methods

The snowflake-like ZnO structures were grown in aqueous solutions at a low temperature. The typical procedure was to use zinc nitrate ($Zn(NO_3)_2$) and hexamethyltetramine ($C_6H_{12}N_4$) mixed solutions with the addition of NaF. The typical reaction process was listed as follows: 0.05 M $Zn(NO_3)_2$ and 0.02 M NaF were dissolved in distilled water. Then, 0.05 M $C_6H_{12}N_4$ was added slowly under stirring condition. Afterward, the mixture solutions were reacted at 90 °C for 5 h. After washing with distilled water and pure ethanol, the sample was dried at 60 °C. Then, the obtained ZnOHF intermediate was baked at 400 °C for 2 h.

* Correspondence: eeywang@gmail.com; yunaisen@126.com

²National Key Laboratory on High Power Semiconductor Lasers, Changchun University of Science and Technology, Changchun 130022, China

³Liaoning Key Laboratory of Optoelectronic Films and Materials, School of Physics and Materials Engineering, Dalian Nationalities University, Dalian 116600, China

Full list of author information is available at the end of the article

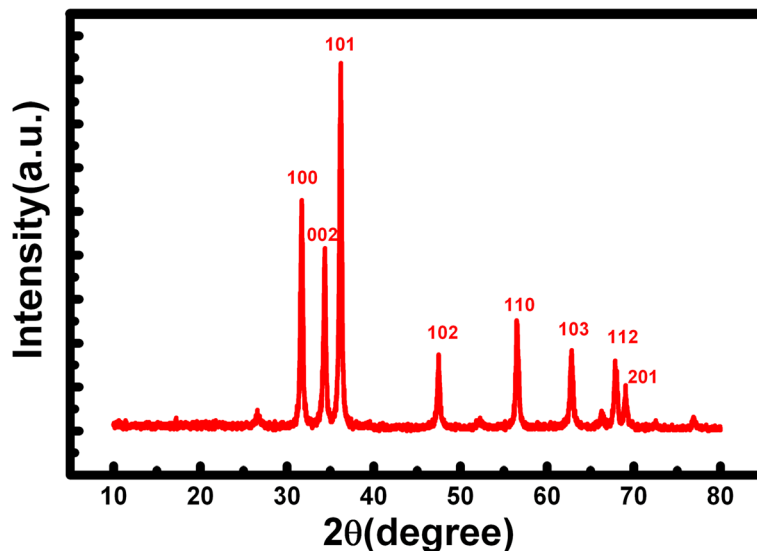


Fig. 1 XRD patterns of the ZnO prepared by a hydrothermal method after the heat treatment

Finally, the as-grown ZnO samples were cleaned with deionized water and dried in the air.

The gas-sensing properties were performed by using a static state gas-sensing measurement system. As-prepared ZnO nanostructures were dispersed with deionized water to form a paste. Afterwards, it was coated onto a ceramic substrate. In addition, three pairs of gold interdigital electrodes were made to form a ZnO sensing film. The thickness of the ZnO sensing film was about 300 nm.

Results and Discussion

Figure 1 shows the XRD results of the ZnO samples. It can be clearly seen that all the diffraction peaks could be attributed to the ZnO wurtzite hexagonal phase. Meanwhile, no impurity peaks are detected, which indicates the high purity of the ZnO.

Figure 2a, b displays a low-magnified morphology of the sample over a large area. It can be clearly seen that the sample was consisted of monodisperse snowflake-

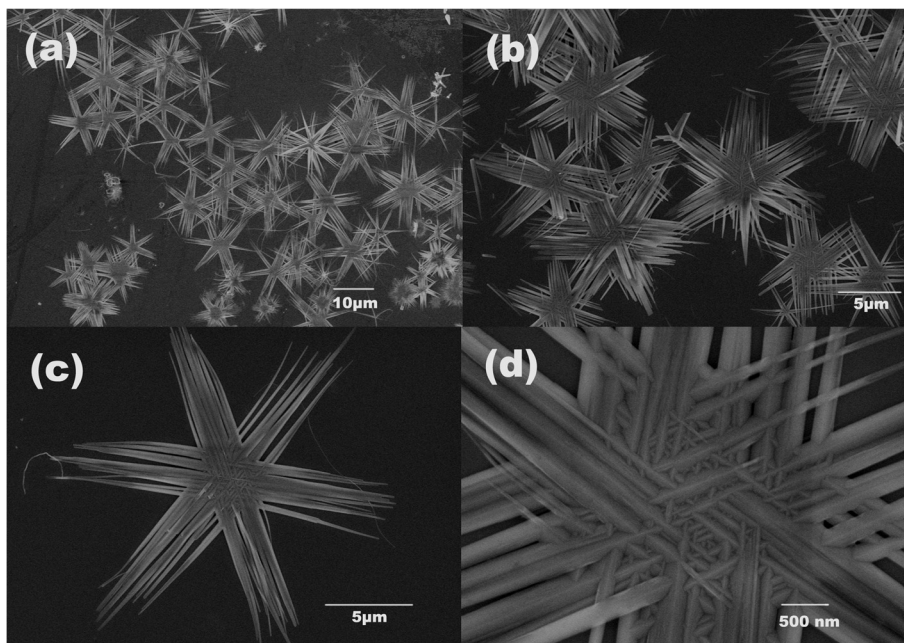


Fig. 2 FESEM images of the as-synthesized ZnO nanostructures. **a** Panoramic view. **b** Enlarged part of the sample. **c** Individual ZnO snow-like structure. **d** Further magnification of a single ZnO snow-like structure

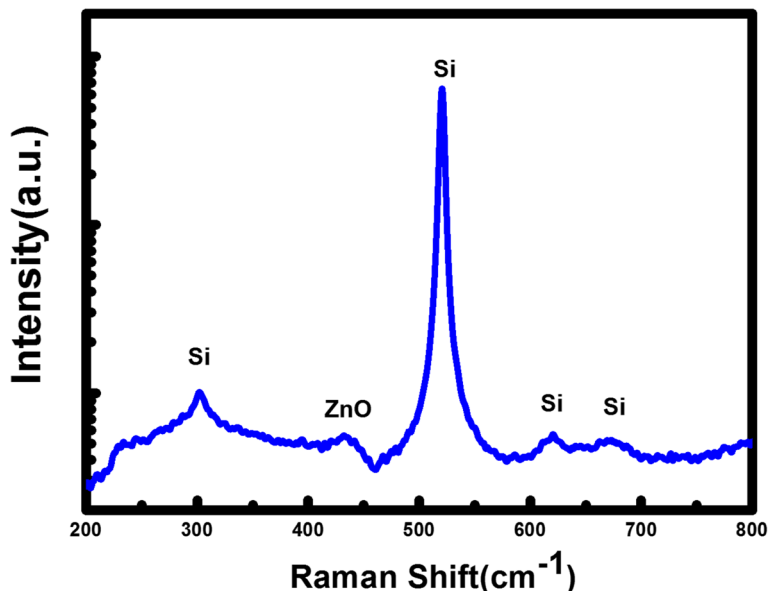


Fig. 3 Micro-Raman spectrum of an as-grown individual ZnO structure

like microstructures. The diameter is around 15 μm , and almost all of them have a uniform size and present one kind of structure. The further magnified pictures are shown in Fig. 2c, d; it can be seen that the nanowires are joining with each other, and a network structure has been formed by interconnected nanowires. The SEM images indicate the formation of snow-shaped hierarchical ZnO architecture. The hierarchical ZnO architecture is found to be made up of nanowires which were self-assembled to form snowflake-shaped assemblies. The

synthesis of hexagonal ZnO nanostructures has been reported [27]. However, the approach based on the solution method to prepare this structure is rarely disclosed. The reason why the structures grow into hexagonal symmetry could be attributed to the hexagonal symmetry of the ZnO core. The ZnO core provides its six prismatic crystal planes facets, which serve as growth platforms for nanowire units. Moreover, the mechanism of forming snowflake-like ZnO structures can be attributed to NaF, and it can react with $\text{Zn}(\text{NO}_3)_2$ to form ZnOHF

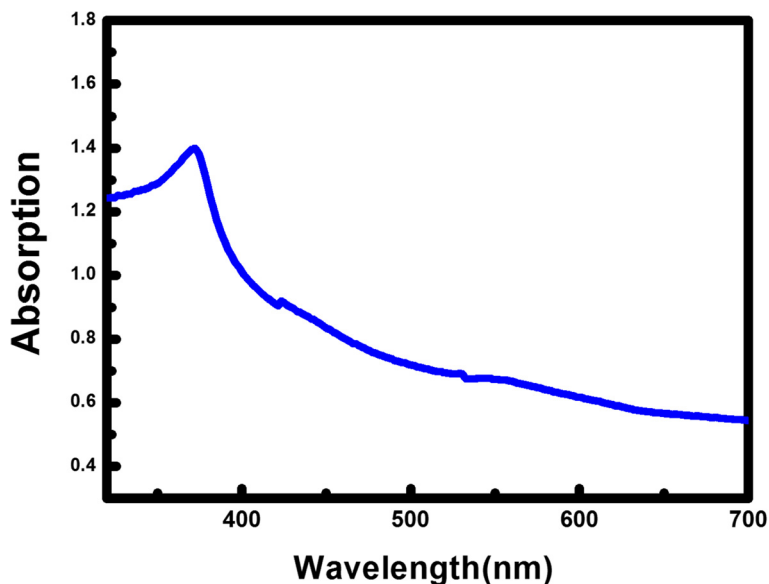


Fig. 4 Absorption spectrum of an as-grown ZnO structure

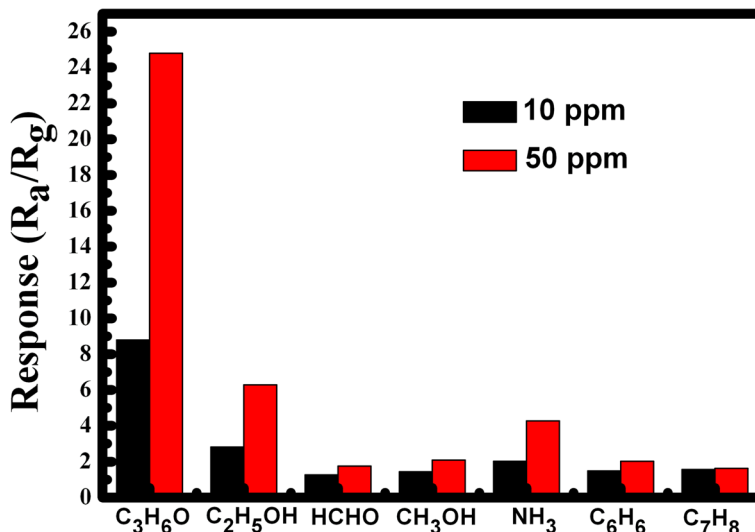


Fig. 5 Response of ZnO nanostructures to 10 and 50 ppm various gases at 350 °C

intermediate. Meanwhile, it can accelerate nanowires that are weaved into netlike structures that overlap with each other [28]. The reaction process of the ZnOHF intermediate could be proposed as follows:

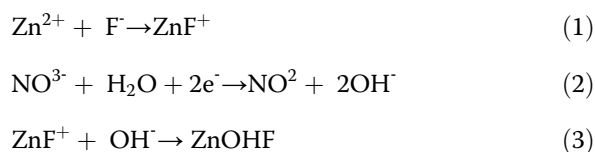


Figure 3 shows the micro-Raman spectrum of an as-grown individual ZnO structure which was dipped on Si. The peak located at 303, 620, and 670 cm⁻¹ are Si

vibration modes [29]. The peak with a weak intensity at 434 cm⁻¹ can be attributed to E₂(H) mode, which are the intrinsic characteristic of the Raman active mode of wurtzite hexagonal ZnO [30]. Meanwhile, it downshifts in comparison with the stress-free bulk ZnO value of 437 cm⁻¹, indicating that it suffers from tensile stress.

Figure 4 displays the absorption spectrum of an as-grown ZnO structure. It shows a strong UV absorption and a weak visible light absorption. Meanwhile, the cut-off wavelength is around 377 nm, which shows a 3-nm blue shift in comparison with the ZnO bulk material (380 nm). This shift corresponds to the quantum confinement effects of nanostructures [31].

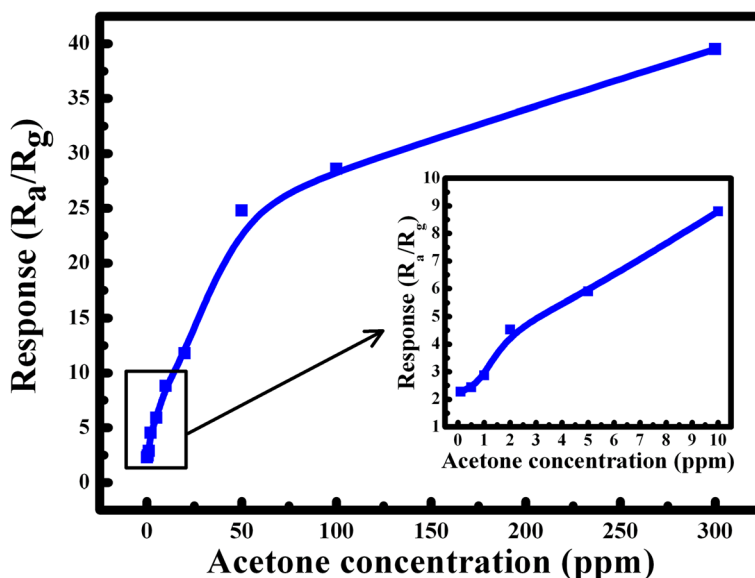


Fig. 6 Response to different concentrations of acetone at an operating temperature of 350 °C

The gas-sensing properties were performed by using a static state gas-sensing measurement system [32]. The as-prepared ZnO nanostructures were coated onto a ceramic substrate (250~300 μm in thickness), dried at 100 $^{\circ}\text{C}$ for 2 h, and annealed at 500 $^{\circ}\text{C}$ for 2 h in air. Finally, a Ni-Cr heating wire was inserted into the ceramic tube to form an inside-heated gas sensor. Voltage division circuit was adopted to measure the export voltage on the sensor. Meanwhile, an external resistor (R_L) was connected in series with the obtained sensor under the bias of 10 V. The gas response value (S) was defined as a ratio of the electrical resistance of the sensor in air (R_a) to that in a testing gas (R_g): $S = R_a/R_g$, and $R_a = R_L(10 - V_{\text{air}})/V_{\text{air}}$, $R_g = R_L(10 - V_{\text{gas}})/V_{\text{gas}}$, where V_{air} was the export voltage of R_L in air and V_{gas} was the voltage in the testing gas [32].

The gas responses of ZnO nanostructures to various testing gases of 10 and 50 ppm are performed with an operating temperature of 350 $^{\circ}\text{C}$. Figure 5 exhibits the histogram showing the response of ZnO sensor to various gas vapours, including acetone ($\text{C}_3\text{H}_6\text{O}$), ethanol ($\text{C}_2\text{H}_5\text{OH}$), formaldehyde (HCHO), methanol (CH_3OH), ammonia (NH_3), benzene (C_6H_6), and methylbenzene (C_7H_8). It can be clearly seen that acetone displayed remarkable higher responses in comparison to the other gases. Under the gas concentrations at 10 ppm, the highest response of the sensor is around 9 to acetone, and those of the other gases are no greater than 3. Moreover, the response to acetone is particularly stronger than the other gases under the gas concentrations at 50 ppm, the response magnitude was about 25, while the response to other gases was no more than 7. It is obvious that the sensor based on snow-like structures exhibits excellent acetone sensing.

Figure 6 demonstrates the concentration-dependent sensitivity of the ZnO sensor based on snow-like structures for acetone detection with an operating temperature of 350 $^{\circ}\text{C}$. It can be seen that the response below 10 ppm acetone increases quickly when the gas concentration is increasing. Above 10 ppm, the response slowly increases with increasing acetone gas concentration. Moreover, the inset in Fig. 6 shows the linear curve below 10 ppm. It indicates the ZnO nanostructures are much more suitable to detect acetone with a low concentration.

The working mechanism of ZnO gas sensors can be attributed to the conductivity changes. The reaction between the testing gas and the oxygen species located on the surface of the ZnO structures could cause resistance change. In our case, when the sensor based on snow-like structures is exposed to acetone gas, the acetone gas is oxidized by the oxygen species to form formaldehyde and then increase conductance. The response to acetone with a low concentration could be ascribed to the snow-like sensor structure, which has a much bigger specific surface area than other conventional sensing structures,

which could provide a larger adsorption region then increase the amount of gas molecules adsorbed on the sample surface. Moreover, the formation of nanowire junctions may be another reason for the response enhancement [33]. The junctions are considered as the active sites, which can increase the gas response sensitivity.

Conclusions

In summary, snowflake-like ZnO structures were synthesized by a simple low-temperature way. The structures are constructed of high-aspect-ratio ZnO nanowires. Moreover, the snowflake-like structure sensor exhibits excellent acetone sensing, which are much suitable to detect acetone with a low concentration.

Acknowledgements

This work was supported by the National Science Foundation of China (Grant No. 51102036, 11474045, 11474036, 61370043), Fundamental Research Funds for the Central Universities DC201502080201, and The Opening Project of State Key Lab of Silicon Materials of Zhejiang University (No. SKL2014-8).

Authors' Contributions

ZC carried out the experiment and drafted the manuscript. YW and ZL commented on the results and revised the manuscript. NY helped in the SEM and gas-sensing characterization. All authors read and approved the final manuscript.

Competing Interests

The authors declare that they have no competing interests.

Author details

¹College of Optoelectronic Engineering, Changchun University of Science and Technology, Changchun 130022, China. ²National Key Laboratory on High Power Semiconductor Lasers, Changchun University of Science and Technology, Changchun 130022, China. ³Liaoning Key Laboratory of Optoelectronic Films and Materials, School of Physics and Materials Engineering, Dalian Nationalities University, Dalian 116600, China.

Received: 22 May 2016 Accepted: 21 July 2016

Published online: 26 July 2016

References

- Xu CX, Sun XW (2003) Field emission from zinc oxide nanopins. *Appl Phys Lett* 83:3806–3808
- Chen SW, Khor OK, Liao M, Chung CK (2014) Sensitivity evolution and enhancement mechanism of porous anodic aluminum oxide humidity sensor using magnetic field. *Sens Actuators B* 199:384–388
- Wang ZL, Song J (2006) Piezoelectric nanogenerators based on zinc oxide nanowire arrays. *Science* 312:242–246
- Lu S, Qi J, Liu S, Zhang Z, Wang Z, Lin P, Liao Q, Liang Q, Zhang Y (2014) Piezotronic interface engineering on ZnO/Au-based Schottky junction for enhanced photoresponse of a flexible self-powered UV detector. *ACS Appl Mater Interfaces* 6:14116–14122
- Chen YR, Hu LQ, Song H, Jiang H, Li DB et al (2014) Optimized performances of tetrapod-like ZnO nanostructures for a triode structure field emission planar light source. *Nanoscale* 6:13544–13549
- Chen YR, Jiang H, Li DB, Song H, Li ZM, Sun JX, Miao GQ, Zhao HF (2011) Improved field emission performance of carbon nanotube by introducing copper metallic particles. *Nano Res Lett* 6:537
- Li S, Zhang T, Wu J et al (2013) Polarization induced hole doping in graded Al_xGa_{1-x}N ($x = 0.7 \sim 1$) layer grown by molecular beam epitaxy. *Appl Phys Lett* 102:062108
- Li S, Ware M, Wu J, Minor P, Wang ZM, Wu ZM, Jiang YD, Salamo JG (2012) Polarization induced pn-junction without dopant in graded AlGa_N coherently strained on GaN. *Appl Phys Lett* 101:122103

9. Wang MJ, Li S, Zhang P, Wang YF, Li HQ, Chen Z (2015) A modified sequential method used to prepare high quality perovskite on ZnO nanorods. *Chem Phys Lett* 639:283–288
10. Pradel KC, Wu W, Zhou Y, Wen X, Ding Y, Wang ZL (2013) Piezotronic effect in solution-grown p-type ZnO nanowires and films. *Nano Lett* 13:2647–2653
11. Ren L, Tian TT, Li YZ, Huang JG, Zhao XJ (2013) High-performance UV photodetection of unique ZnO nanowires from zinc carbonate hydroxide nanobelts. *ACS Appl Mater Interfaces* 5:5861–5867
12. Deng JN, Yu B, Lou Z, Wang LL, Wang R, Zhang T (2013) Facile synthesis and enhanced ethanol sensing properties of the brush-like ZnO–TiO₂ heterojunctions nanofibers. *Sensors and Actuators B* 184:21–26
13. Li DB, Sun XJ, Song HZM, Chen YR, Jiang H, Miao GQ (2012) Realization of a high-performance GaN UV detector by nanoplasmonic enhancement. *Adv Mater* 24:845–849
14. Xie W, Li YZ, Shi WQ, Zhao L, Zhao XJ, Peng PF, Wang SJ (2012) Novel effect of significant enhancement of gas-phase photocatalytic efficiency for nano ZnO. *Chem Eng J* 213:218–224
15. Pawar RC, Shaikh JS, Shewale PS, Patil PS (2011) Characterization of zinc oxide nanoparticles synthesized by polymer assisted deposition method. *J Alloys Compd* 509:1716–1721
16. Xu JQ, Chen YP, Chen DY, Shen JN (2006) Hydrothermal synthesis and gas sensing characters of ZnO nanorods. *Sens Actuators B* 113:526–531
17. Chen LF, Song H, Cao LZ, Jiang H, Li DB, Guo WG, Liu X, Zhao HF, Li ZM (2009) Effect of interface barrier between carbon nanotube film and substrate on field emission. *J Appl Phys* 106:033703
18. Wang J, Wei XW, Wangyang PH (2015) Gas-sensing devices based on Zn-doped NiO two-dimensional grainy films with fast response and recovery for ammonia molecule detection. *Nanoscale Res Lett* 10:461
19. Liu JY, Zhang Y, Liu CH, Peng MZ, Yu AF, Kou JZ, Liu W, Zhai JY, Juan L (2016) Piezo-phototronic effect enhanced UV photodetector based on CuI/ZnO double-shell grown on flexible copper microwire. *Nanoscale Res Lett* 11:281
20. Qin XS, Li GJ, Xiao L, Chen GZ, Wang K, Wang Q (2016) Effect of oxidation condition on growth of N: ZnO prepared by oxidizing sputtering Zn-N film. *Nanoscale Res Lett* 11:274
21. Zhang P, Li S, Liu CH, Wei XB, Wu ZM, Jiang YD, Chen Z (2014) Near-infrared optical absorption enhanced in black silicon via Ag nanoparticle-induced localized surface plasmon. *Nanoscale Res Lett* 9:519
22. Sohn JI, Jung YI, Baek SH, Cha S, Jang JE, Cho CH et al (2014) A low temperature process for phosphorous doped ZnO nanorods via a combination of hydrothermal and spin-on dopant methods. *Nanoscale* 6:2046–2051
23. Xi Y, Hu CG, Han XY, Xiong YF, Gao PX, Liu GB (2007) Hydrothermal synthesis of ZnO nanobelts and gas sensitivity property. *Solid State Commun* 141:506–509
24. Shi RX, Yang P, Dong XB, Ma Q, Zhang AY (2013) Growth of flower-like ZnO on ZnO nanorod arrays created on zinc substrate through low-temperature hydrothermal synthesis. *Appl Surf Sci* 264:162–170
25. Fan HQ, Jia XH (2011) Selective detection of acetone and gasoline by temperature modulation in zinc oxide nanosheets sensors. *Solid State Ion* 192:688–692
26. Wen BM, Huang YZ, Boland JJ (2008) Controllable growth of ZnO nanostructures by a simple solvothermal process. *J Phys Chem C* 112:106–111
27. Lao JY, Wen JG, Ren ZF (2002) Hierarchical ZnO nanostructures. *Nano Lett* 2:1287–1291
28. Yu NS, Zhao HF, Zhang LG, Hu DY, Ma XY, Dong B (2014) Synthesis of ZnO nanowires on aluminum flake by aqueous method. *Applied Physics A* 114:1209–1213
29. Yang B, Kumar A, Feng P, Katiyar RS (2008) Structural degradation and optical property of nanocrystalline ZnO films grown on Si (100). *Appl Phys Lett* 92:233112–233114
30. Decremps F, Porres JP, Saitta AM, Chervin JC, Polian A (2002) High-pressure Raman spectroscopy study of wurtzite ZnO. *Physical Review B* 65:092101
31. Wu L, Wu Y, Pan X, Kong F (2006) Synthesis of ZnO nanorod and the annealing effect on its photoluminescence property. *Opt Mater* 28:418–422
32. Du HY, Wang J, Yao PJ, Hao YW, Li XG (2013) Preparation of modified MWCNTs-doped PANI nanorods by oxygen plasma and their ammonia-sensing properties. *J Mater Sci* 48:3597–3604
33. Zhang DH, Liu ZQ, Li C, Tang T, Liu XL, Han S, Lei B, Zhou CW (2004) Detection of NO₂ down to ppb levels using individual and multiple In₂O₃ nanowire devices. *Nano Lett* 4:1919–1924

Submit your manuscript to a SpringerOpen[®] journal and benefit from:

- Convenient online submission
- Rigorous peer review
- Immediate publication on acceptance
- Open access: articles freely available online
- High visibility within the field
- Retaining the copyright to your article

Submit your next manuscript at ► springeropen.com
